Plasma Chem Plasma Process (2011) 31:291–306
DOI 10.1007/s11090-010-9281-0

ORIGINAL PAPER

Oxidative Conversion of Hexane to Olefins-Influence of Plasma and Catalyst on Reaction Pathways

C. Boyadjian · A. Ağıral · J. G. E. Gardeniers · L. Lefferts · K. Seshan

Received: 20 July 2010 / Accepted: 16 December 2010 / Published online: 3 February 2011

Abstract An integrated plasma-Li/MgO system is efficient for the oxidative conversion of hexane. In comparison to the Li/MgO catalytic system, it brings considerable improvements in the yields of light olefins ($C_2^=$–$C_5^=$) at relatively low temperatures indicating synergy from combination of plasma and catalyst. The study on the influence of temperature on the performance of the integrated plasma-Li/MgO system shows dominancy of plasma chemistry at the lower temperature (500°C), while contribution from the catalyst both in hexane activation and in enhancing olefin formation becomes significant at the higher temperature (600°C). At 500°C significant amount of acetylene formation is observed. This is minimized at 600°C at oxygen depleting conditions.

Keywords Barrier discharge · Plasma · Hexane · Oxygen · Oxidative conversion · Olefins · Oxicracking · Li/MgO

Introduction

Catalytic oxidative cracking of naphtha is conceptually a potential alternative process to steam cracking. Both the presence of oxygen and catalyst are beneficial for facilitating cracking reactions at lower temperatures. Reactions in presence of oxygen are exothermic, thus internally provide heat for endothermic cracking reactions (C–C, C–H bond cleavage). Presence of catalyst stimulates C–C, C–H bond scission in the alkane and induces cracking at lower temperatures than in the homogeneous phase. The development of an efficient oxidation catalyst that minimizes combustion, however, remains a challenge. Recent studies on oxidic catalysts with no facile red-ox properties have shown tremendous

C. Boyadjian · L. Lefferts · K. Seshan (✉)
Catalytic Processes and Materials, MESA+ Institute for Nanotechnology, Faculty of Science and Technology, University of Twente, P.O. Box 217, 7500 AE Enschede, The Netherlands
e-mail: k.seshan@tnw.utwente.nl

A. Ağıral · J. G. E. Gardeniers
Mesoscale Chemical Systems, IMPACT, MESA+ Institute for Nanotechnology, Faculty of Science and Technology, University of Twente, P.O. Box 217, 7500 AE Enschede, The Netherlands

increase in olefin yields [1, 2]. Among these is the Li/MgO catalyst, which has been extensively studied in literature for the oxidative conversion of alkanes; oxidative coupling of methane [3, 4] and oxidative dehydrogenation/cracking of ethane [5, 6], propane and butane [7–11]. Unlike in the case of oxidic catalysts with red-ox properties [12], sequential combustion of olefins over Li/MgO occurs to a minimal extent, resulting in an olefin selectivity which is almost invariant with the alkane conversion levels. Recently, we [13] reported on the performance of Li/MgO catalyst for the oxidative conversion/cracking of hexane. The catalyst showed very good selectivity to C_2–C_4 olefins (60 mol %) at a temperature as low as 575°C, which is much lower than temperatures used in steam crackers ($T \geq 800$°C). Similar to what is reported in literature and our earlier studies for oxidative conversion of lower alkanes (methane [3], ethane [4–6, 12], propane [6–11] and butane [7]), we proposed hexane activation via the $[Li^+O^-]$ sites of Li/MgO abstracting $H^\bullet$. The hexyl radical formed then undergoes complex radical chemistry in gas phase in presence of molecular oxygen, forming the product mixture of C_1–C_5 products, including olefins, paraffins and combustion (CO_x) products.

Li/MgO has no cations with variable valency and unlike catalysts with red-ox properties ($Mn^{2+,3+}$, $Co^{2+,3+}$), has lower oxidation activity. This results in relatively low hexane conversions during the oxidative cracking of hexane [13]. Kinetic results from the oxidative conversion of alkanes over the Li/MgO show that C–H bond splitting is the rate limiting step in these reactions [9]. Even in the presence of strong $H^\bullet$ abstractor, e.g., $[Li^+O^-]$, high temperatures ≥550°C are still required to induce this step.

In an attempt to enhance the $H^\bullet$ abstraction in the alkane, we recently investigated the oxidative conversion of propane [14, 15], ethane and methane [14] at ambient conditions in presence of plasma in a micro-reactor both in presence and absence of Li/MgO catalyst. Indeed, in these experiments plasma induced alkane activation and alkyl radicals were formed at ambient conditions as result of electron impact collisions caused by plasma. In the case of propane plasma experiments, higher conversions were observed in the presence of Li/MgO catalyst as compared to empty micro-reactor. This is due to enhanced plasma efficiency as result of increase in permittivity of the system, leading to increase in electron density, hence electron impact collisions [15]. The presence of Li/MgO catalyst also resulted in enhanced selectivity to propylene. Propyl radicals, generated from propane via activation by plasma, interact with the $[Li^+O^-]$ sites of the catalyst, where the latter abstracts a second hydrogen atom from the propyl radical forming propylene [15].

Recently, we [16] investigated the oxidative conversion of hexane in a plasma reactor in the temperature range 400–600°C. Similar to lower alkanes, the application of plasma induced hexane and oxygen conversion at temperatures as low as 400°C. At the lower temperatures (400, 500°C) coupling of formed radicals was observed leading to formation of C_6^+ hydrocarbons. However, at the higher temperature (600°C) cracking and lower olefins ($C_2^=$–$C_4^=$) formation became more significant. Optimum olefins yields were observed at 8% of oxygen in the feed, as increasing oxygen concentrations above this resulted in the formation of combustion products.

Although application of non-thermal plasma (plasma at ambient conditions) is more commonly reported, integrated plasma-catalytic systems at elevated temperatures, so-called plasma/catalysis have also been of continuous interest, especially for decomposition of hydrocarbons [17, 18]. In particular, decomposition of methane to hydrogen and carbon has been investigated [19, 20]. Nozaki et al. [20], investigated steam reforming of methane using plasma with a Ni/SiO_2 catalyst. A strong synergistic effect and hence significant improvement in the methane conversion was observed at 400°C. Similarly, the

presence of catalyst downstream to plasma, during the oxidative conversion of methane [21], improved selectivities to ethylene.

In analogy to such systems, in the present work the performance of an integrated plasma-Li/MgO system for the oxidative conversion of hexane is reported. Our objective is to further enhance the yields of olefins, compared to those achieved in the plasma reactor in the absence of the catalyst. The influence of plasma on the selectivities to various products in relation to the chemistry on the surface; i.e., the role of Li/MgO catalyst in hexane activation and controlling olefin formation, is discussed.

Experimental

Materials and Methods

Commercially available $Mg(OCH_3)_2$ solution in methanol (Aldrich, 6-8wt% in methanol), CH_3OH (Merck), $LiNO_3$ (Aldrich, assay $\geq$99.99%) were used for preparation of Li/MgO catalysts. Sol–gel synthesized Li/MgO catalyst used in this study was prepared according to the method described earlier by us [10].

BET surface area of the catalyst was determined with nitrogen physisorption using a Micro-metrics Tristar instrument. The samples were out-gassed in vacuum at 250°C for 24 h prior to the analysis. BET surface area of the catalyst was 82 m^2/g. The elemental composition of the catalyst was determined with atomic absorption spectroscopy (AAS). Li content in the catalyst was 0.86 wt%.

Catalytic Measurements

Measurements with the integrated plasma-Li/MgO system were carried out at atmospheric pressure and isothermal conditions in a fixed-bed reactor [16]. A quartz reactor of 4 mm internal diameter was used. The reactor was equipped with an internal stainless steel wire (ID 1.5 mm) as high voltage electrode and an external aluminum foil as ground electrode. Plasma was generated between the high voltage wire electrode and the grounded aluminum foil around the quartz tube using 6 kV peak AC voltage. The power supply had an output of 10 Watts maximum. The power absorbed by the plasma was calculated to be $\sim$3 W (180 J/min). This was evaluated using the corresponding V-Q Lessajous figures, obtained using an oscilloscope [19]. Light emission from the discharge was collected through a collimating lens placed at a 90^o angle to the outside of the reactor. An optical fiber was used to transmit the light to an optical emission spectrometer (HR 4000, Ocean Optics).The HR 4000 spectrometer was responsive from 200 to 1,100 nm with a resolution of 0.04 nm.

Catalyst or quartz particles (300–500 mg depending on the experiment) were packed between two quartz-wool plugs in the quartz reactor according to configuration in Fig. 1a. For gas phase non-catalytic reactions, an empty reactor according to configurations in Fig. 1b, c were used. A different reactor configuration with Li/MgO downstream to plasma (Fig. 1d) was as well investigated. Powder catalyst was pressed, crushed and sieved to particle size range of 0.4–0.6 mm before use. Reactions were studied at both 500 and 600°C. The reactor was heated using an electrical furnace. The temperature of the furnace was controlled by a thermocouple placed outside the reactor tube within the isothermal zone of the tubular furnace. Total gas feed of 100 ml/min was used. This consisted of 10 mol% of hexane vapor, 8 mol% of oxygen and balance helium. Before each catalytic test, the catalyst was pretreated in 50%O_2/He (60 ml/min) for 1 h at a temperature of

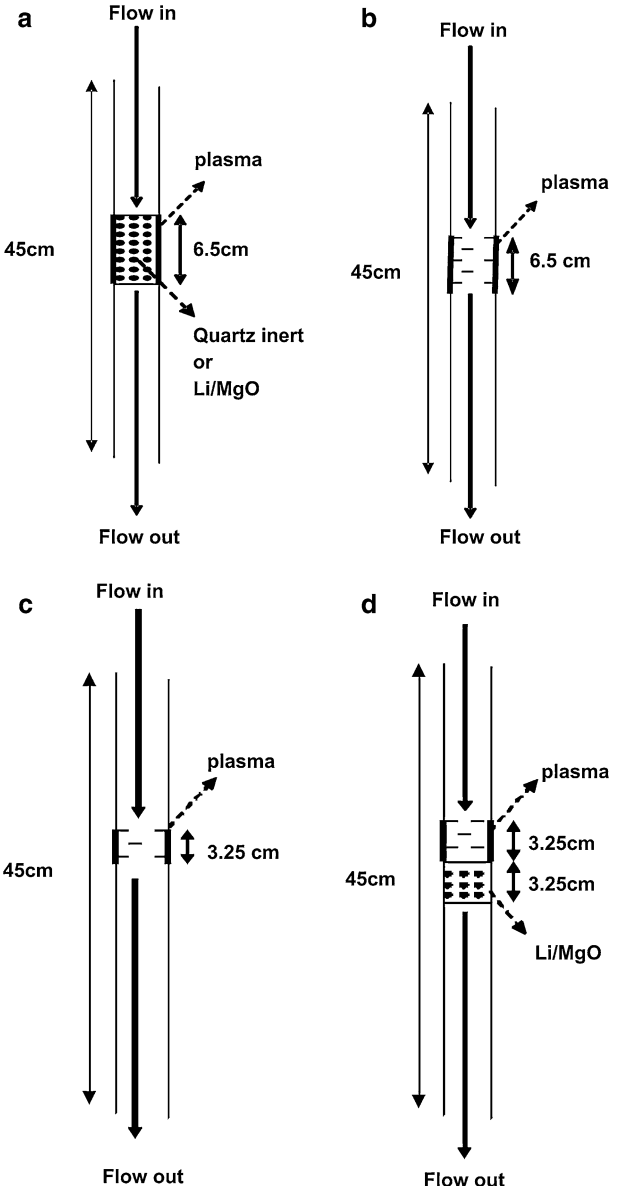

Fig. 1 Reactor configurations used; Plasma applied to Li/MgO (P_Li/MgO) or quartz (P_Quartz) (**a**), plasma applied to empty reactor (P_ER) (**b**, **c**), and Li/MgO downstream to plasma zone (PB_Li/MgO) (**d**)

650°C. For analysis of the product mixture two online micro GCs were utilized. The experimental setup used for catalyst testing and analysis details are described in [13].

Hexane conversions were calculated on carbon mol basis; i.e., (C_6^{in} moles–C_6^{out} moles)/C_6^{in} moles × 100%. The carbon balance closed between 100 and 110%. Selectivity to individual products was also calculated based on the number of moles of carbon contained in the products.

Results and Discussion

Figure 2 shows hexane conversions from the oxidative conversion of hexane both at 500 and 600°C, (1) in an empty reactor in the absence and presence of plasma and (2) with Li/MgO catalyst without plasma. Gas phase activation of hexane in the empty reactor and in absence of plasma, occurs via thermal cleavage of C–C and C–H bonds leading to radical formation and/or via collision of hexane with oxygen molecules forming hexyl ($C_6H_{13}^{\bullet}$) and $HO_2^{\bullet}$ radicals. The latter act as the main chain propagators in the gas phase radical chemistry [13, 16]. At both temperatures hexane conversions in the empty reactor were almost negligible. The introduction of the catalyst however, resulted in a considerable improvement in hexane conversions. Significantly, the application of plasma enhanced hexane conversions at both temperatures.

Thus, results of hexane conversions in Fig. 2 elucidate the significant influence of both Li/MgO catalyst and plasma on hexane activation. Temperature has also a clear effect on hexane conversions but was more significant in the case of the Li/MgO catalyst. Details of the oxidative conversion of hexane in the presence of both (1) plasma and (2) Li/MgO catalyst at 500 and 600°C are presented in sections below.

Oxidative Conversion of Hexane in the Presence of Plasma

During the oxidative conversion of hexane, we previously showed that the role of plasma was to induce both hexane and oxygen conversions via electron impact excitations. The average electron energy for the 'hexane + oxygen + helium' system, solving the Boltzmann distribution [16], was calculated to be 4.3 eV. This is sufficient to induce C–C (bond energy 3.17 eV) and C–H (bond energy 3.97 eV) bond scission in the hexane, and the fraction of electrons with higher energy can also cause dissociation of molecular oxygen ($\sim$6 eV). The dramatic improvement observed [16] in hexane conversions with the introduction of oxygen in the system, confirmed the existence of new routes for hexane

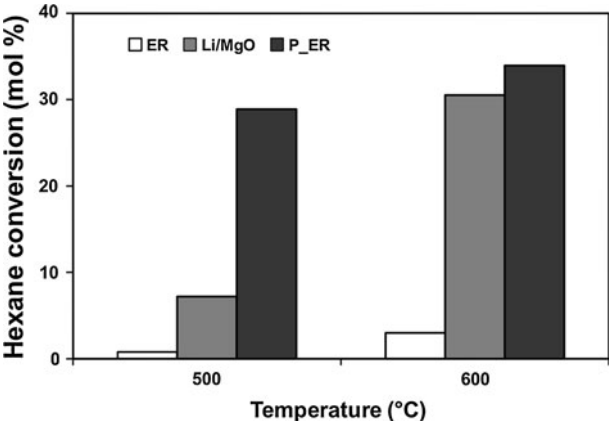

Fig. 2 Hexane conversions (1) in an empty reactor, (2) with Li/MgO and (3) in a plasma reactor. Oxygen conversions (mol%): At 500°C; 4 (ER), 56 (Li/MgO), 71 (P_ER) and at 600°C; 10 (ER), 100 (Li/MgO), 100 mol% (P_ER). Reaction conditions: 100 ml/min, 10% hexane, 8% oxygen and balance helium. WHSV (weight hourly space velocity) = 3.08 h^{-1}

conversion, involving gas phase activation of oxygen by plasma. Calculation of the fractional energy dissipated in the electron impact processes leading to vibrational excitation, ionization and dissociation of both hexane and oxygen molecules showed that dissociation of these molecules is a more significant pathway [16]. Thus, in the presence of plasma the following hexane dissociation routes were proposed (2) C–C, C–H bond scission by electron-impact excitation of hexane molecules (1–4) and (3) C–H bond scission by collision of hexane molecules with $O(^3P)$ oxygen atoms (5) formed from electron impact excitations of molecular oxygen (6–7). Moreover, we showed previously [16], the reaction of molecular oxygen with hexyl radicals forming $HOO^{\bullet}$ radicals (8). $HOO^{\bullet}$ radicals act as the main chain propagators and increase the radical concentration during oxidative conversion.

$$C_6H_{14} + e^- \rightarrow C_6H_{13}^{\bullet} + H^{\bullet} + e^- \quad (1)$$

$$C_6H_{14} + e^- \rightarrow C_5H_{11}^{\bullet} + CH_3^{\bullet} + e^- \quad (2)$$

$$C_6H_{14} + e^- \rightarrow C_4H_9^{\bullet} + C_2H_5^{\bullet} + e^- \quad (3)$$

$$C_6H_{14} + e^- \rightarrow C_3H_7^{\bullet} + C_3H_7^{\bullet} + e^- \quad (4)$$

$$C_6H_{14} + O(^3P) \rightarrow C_6H_{13}^{\bullet} + OH^{\bullet} \quad (5)$$

$$O_2 + e^- \rightarrow 2O(^3P) + e^- \quad (6)$$

$$O_2 + e^- \rightarrow O(^3P) + O(^1D) + e^- \quad (7)$$

$$O_2 + C_6H_{13}^{\bullet} \rightarrow C_6H_{12} + HOO^{\bullet} \quad (8)$$

Optical emission spectrum of a C_6H_{14}–He mixture in plasma (Fig. 3) confirms the influence of plasma on hexane activation. Features of the electronic excitation of the $CH^{\bullet}$ radical corresponding to the $A^2\Delta \rightarrow X^2\pi$ transition at 431.15 nm and bands corresponding to $H^{\bullet}$ radicals (656.05 nm) (Hα, Balmer series) and helium (587.61 and 667.78 nm) were observed. The existence of CH and H bands in the optical emission spectrum of C_6H_{14}-He mixture indicate the decomposition of hexane in plasma via C–H and C–C bond cleavage. $CH^{\bullet}$ radicals in the presence of plasma are generally formed, as proposed in literature by Kado et al. [22], through the extensive dehydrogenation of methyl radicals via multiple electron impact excitations (9–10) and/or from the coupling of atomic C and H radical (11) formed through extensive dissociation of methane (12).

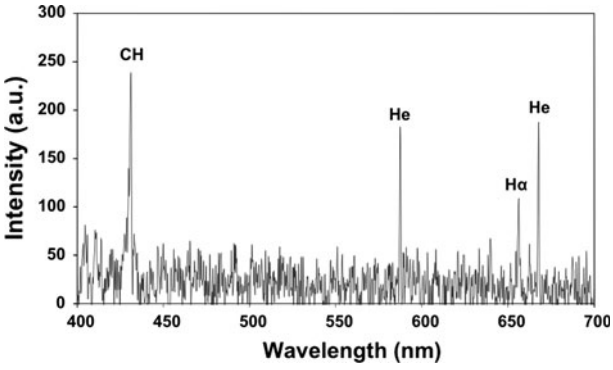

Fig. 3 Optical emission spectrum for a gas mixture of 10% hexane in helium in the presence of plasma at 3 W and at ambient conditions. The HR 4000 spectrometer was responsive from 200 to 1,100 nm with a resolution of 0.04 nm

$$CH_3^{\bullet} + e^- \rightarrow CH_2^{\bullet} + H^{\bullet} + e^- \quad (9)$$

$$CH_2^{\bullet} + e^- \rightarrow CH^{\bullet} + H^{\bullet} + e^- \quad (10)$$

$$C + H^{\bullet} \rightarrow CH^{\bullet} \quad (11)$$

$$CH_4 + e^- \rightarrow C + 4H^{\bullet} + e^- \quad (12)$$

$CH^{\bullet}$ radicals further follow predominantly two reactions; (1) Dimerization of $CH^{\bullet}$ radicals lead to formation of C_2H_2, and (2) reaction with oxygen lead to CO_2. Experiments studying the influence of oxygen concentrations during oxidative conversion of hexane in the plasma reactor [16], showed dramatic decrease in C_2H_2 formation with addition of oxygen in the feed. Since carbon balance in our experiments were relatively good (±10%) and experiments were carried out in the presence of oxygen, it is less likely that $CH^{\bullet}$ is converted to coke. It is essential to note that gas phase radical chemistry is very complex and $CH^{\bullet}$ radicals can also possibly follow various other reaction routes.

Figure 4 presents the selectivities to various products obtained from oxidative conversion of hexane in the plasma empty reactor. Temperature has a clear influence on the product distribution. At 500°C, significant formation of C_6^+ products was observed. These products were not precisely identified at molecular level due to limitation of the micro GCs, but their presence indicates the coupling of the C_1–C_5 radicals subsequent to their formation from dissociation of hexane (13). At 600°C, however, the formation of less C_6^+ products and more C_3–C_5 olefins was observed. This indicates that at this temperature coupling reactions of C_1–C_5 radicals occur to a lesser extent. C–C bond formation is exothermic hence favored at the lower temperatures. In agreement, during the oxidative conversion of methane, ethane and propane in a plasma-micro reactor [14, 15], coupling reactions and formation of hydrocarbons with carbon numbers higher than the feed were observed at lower temperatures.

$$C_xH_{2x+1}^{\bullet} + C_yH_{2y+1}^{\bullet} \rightarrow C_nH_{2n+2} \qquad x, y = 1-5, \quad n = \geq 6 \quad (13)$$

At 500°C, significant formation of acetylene and ethylene and lower amounts of C_3–C_5 olefins was observed (Fig. 4), i.e., $(C_2H_2 + C_2H_4) > (C_3^{=}$–$C_5^{=})$. Acetylene formation is

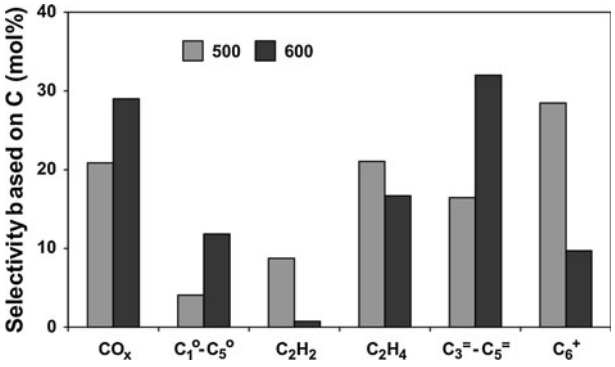

Fig. 4 Effect of temperature on the product distribution of oxidative conversion of hexane in the presence of plasma. Hexane conversions: 29 mol% (500°C) and 31 mol% (600°C). Reaction conditions: 100 ml/min, 10% hexane, 8% oxygen and balance helium

strong evidence of plasma chemistry. Two routes for formation of acetylene have been proposed in literature [16, 20]. In addition to dimerization of $CH^{\bullet}$ radicals discussed above, acetylene is also formed through the extensive dehydrogenation of ethane (14).

$$C_2H_6 \rightarrow C_2H_4 \rightarrow C_2H_2 \tag{14}$$

At 600°C, however, a higher ratio of $(C_3^{=}–C_5^{=})/(C_2H_2+C_2H_4)$ was observed than at 500°C. This indicates that at this temperature the reaction of C_1–C_5 radicals with molecular oxygen to olefins is more favored (15).

$$C_nH_{2n+1}^{\bullet} + O_2 \rightarrow C_nH_{2n} + HOO^{\bullet} \quad n = 1 - 5 \tag{15}$$

Oxidative conversion of hexane over Li/MgO catalyst

In the case of Li/MgO catalyst, $[Li^+O^-]$ defect sites are responsible for catalytic activity [3, 4, 8–11]. Oxidative conversion of hexane, thus, involves hexane activation via homolytic scission of C–H bond on the $[Li^+O^-]$ sites, forming a hexyl radical (16) [13].

$$C_6H_{14} + Li^+O^- \rightarrow C_6H_{13}^{\bullet} + Li^+OH^- \tag{16}$$

Figure 5 shows the product distribution obtained from the oxidative conversion of hexane over Li/MgO catalyst at 500 and 600°C. At 500°C Li/MgO catalyst showed high selectivity to combustion products (75 mol %) and only 21 mol% of total olefins ($C_2^{=}–C_5^{=}$). In the oxidative conversion of lower alkanes/alkenes over MgO, the interaction of hydrocarbons with O^{2-} sites of MgO forming surface alkoxides as precursors for CO_x, has been reported by Aika and Lunsford [23, 24]. Similarly, in the oxidative conversion of hexane over Li/MgO, the high selectivity to combustion products, especially at the low temperature (500°C), has been shown by us [13] to be due to the adsorption of the intermediate radicals on O^{2-} sites of MgO, and their consecutive transformation to CO_x via molecular oxygen. At the higher temperature (600°C), however, cracking and olefin formation were more favored (62 mol% of $C_2^{=}–C_5^{=}$ and 28 mol% of CO_x). This is due to the high temperatures favoring desorption of radicals formed by hydrogen abstraction, and limiting reaction with surface oxygen for alkoxide formation.

Unlike in the presence of plasma, C_2H_2 or C_6^+ products were not observed here. Both at 500 and 600°C selectivities to C_3–C_5 olefins were higher than those to C_2H_4 ($C_3^{=}–C_5^{=} > C_2^{=}$)

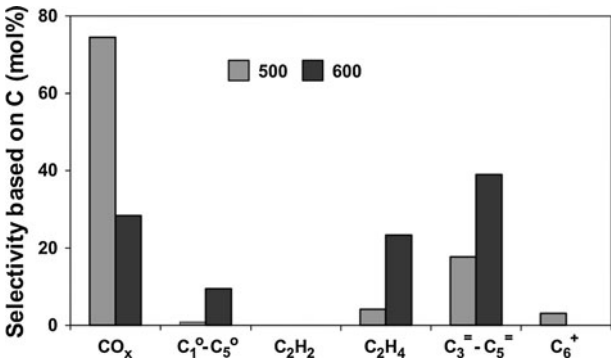

Fig. 5 Effect of temperature on the product distribution of oxidative conversion of hexane over Li/MgO catalyst. Hexane conversions: 7 mol% (500°C) and 31 mol% (600°C). Reaction conditions: 100 ml/min, 10% hexane, 8% oxygen and balance helium. WHSV = 3.08 h^{-1}

which is an indication of role for Li/MgO in cracking and olefin distribution, as homogeneous cracking would yield higher amounts of ethylene than higher olefins ($C_3^=$–$C_5^=$). In the oxidative conversion of hexane over Li/MgO, we proposed, based on experimental results [13] and similar to propositions by Sinev [25], the preference of the [O^-] sites of Li/MgO for hydrogen abstraction from a secondary carbon atom in hexane. This increases the probability of formation of iso-hexyl radicals. β-scission of iso-hexyl radicals yields preferentially more of C_3–C_5 olefins than ethylene.

Oxidative conversion of hexane in the situations discussed so far i.e., (1) in the presence of plasma without catalyst and (2) in the presence of Li/MgO catalyst without plasma, however, yields even at the higher temperature (600°C) limited C_2–C_5 olefins ($\sim$18 mol%) due to formation of CO_x ($\sim$28 mol%). [Li^+O^-] sites have a strong affinity for $H^\bullet$ abstraction, and since presence of plasma (1) enhances formation of hydrocarbon radicals and (2) abstraction of $H^\bullet$ from a hydrocarbon radical leads to olefins, combination of plasma with Li/MgO may be useful. In an attempt to further increase olefin yields, i.e., enhance both hexane conversions and selectivities to total olefins ($C_2^=$–$C_5^=$), the integrated plasma-Li/MgO system is studied for the oxidative conversion of hexane.

Integrated plasma-Li/MgO for the oxidative conversion of hexane

Figure 6 presents hexane conversions in the absence of plasma with Li/MgO catalyst (Li/MgO), and in the presence of plasma in each of the following systems: (1) an empty reactor (P_ER), (2) a reactor packed with catalyst particles (P_Li/MgO) and (3) a reactor packed with quartz inert particles (P_Quartz). Results of experiments with quartz inert particles were included mainly for comparison.

At 500°C the integrated plasma-Li/MgO system resulted in higher hexane conversions than the cumulative conversions achieved with plasma and Li/MgO separately, showing synergy. This effect was not observed at 600°C, due to depletion of oxygen (O_2 conversion = 100%) from reaction stream limiting hexane conversions.

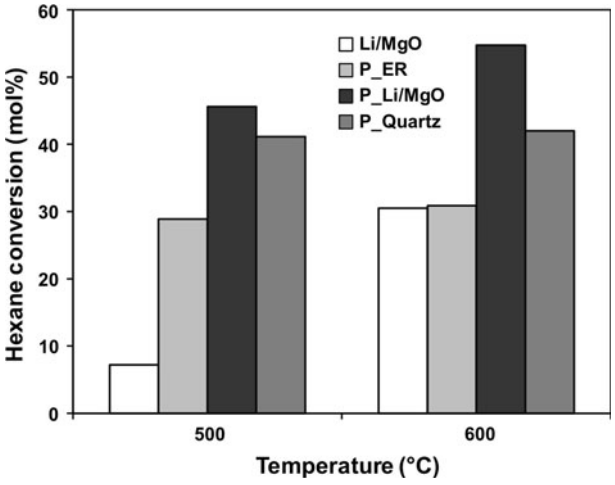

Fig. 6 Hexane conversions with the systems; (1) Li/MgO, (2) P_ER, (3) P_Li/MgO, and (4) P_Quartz. Oxygen conversions (mol %): At 500°C; 56 (Li/MgO), 71 (P_ER), 75 (P_Li/MgO), and 68 (P_Quartz) and at 600°C; 100 (Li/MgO), 100 (P_ER), 100 (P_Li/MgO) and 97 (P_Quartz). Reaction conditions: 100 ml/min, 10% hexane, 8% oxygen and balance helium. WHSV = 3.08 h^{-1}

In order to explain the influence observed we will discuss two propositions: (1) Firstly, it concerns the presence of new [O^-] defect sites on the surface of Li/MgO catalyst created by UV light generated from plasma. Knozinger and co-workers [26], reported, using EPR studies, that monochromatic UV irradiation of MgO particles at 5.4 eV (230 nm) and 4.6 eV (270 nm) leads to the ionization of low-coordinated surface oxygen anions $(O^2_{LC})^-$ in MgO, forming a localized surface hole state [O^-] and a surface-trapped electron. Moreover, they reported [27], that such surface species are as well formed from the polychromatic (200–900 nm) irradiation of MgO with low energy photons (3.9–1.5 eV) resulting in a different dynamics of hole and electron center signals compared to those induced with monochromatic irradiation (282 nm). Thus, based on studies by Knozinger and co-workers [26, 27], we propose that in our helium–oxygen-hexane system, UV light (400–700 nm) generated by plasma, as observed in the optical emission spectrum (Fig. 3), leads to the ionization of the low-coordinated surface oxygen anions $(O^2_{LC})^-$ in MgO, forming a localized surface hole state [O^-] and a surface-trapped electron (17).

$$O^{2-}_{LC} + h\nu \rightarrow O^{-}_{LC} + e^- \tag{17}$$

These [O^-] defect sites created by the plasma, similar to the [Li^+O^-] sites, can also enhance $H^\bullet$ abstraction from hexane forming hexyl radicals. (2) Secondly, we explain the synergistic effect by the accelerated gas phase radical chemistry due to the higher permittivity of Li/MgO (dielectric constant of MgO = 9.7 [28]) in comparison to that of plasma (dielectric constant of plasma <1 [29]) in the empty reactor. The relative permittivity of a dielectric barrier can strongly determine the amount of charge that can be stored for a certain value of applied electric field [30]. The higher the number of charges transferred, the higher is the number of electron impact excitations of hexane molecules [31]. The presence of Li/MgO particles would also, additionally, influence the strength of the electric field. Kang et al. [32] studied the influence of the ferroelectric pellets on the discharge characteristics of dielectric barrier discharges (DBD). They reported that the presence of ferroelectric pellets in plasma can create a non-uniform stronger electric field. This effect created by the packing material, can result in an increase in the average electron energy. Consequently, the number of electron impact dissociations of hexane molecules increases resulting in improved hexane conversions.

Table 1 shows the influence of plasma on the selectivities to various products during the oxidative conversion of hexane over the Li/MgO catalyst. At both temperatures, application of plasma improved the product distribution resulting in a considerable increase in the formation of total olefins ($C_2^=$–$C_5^=$) and a decrease in formation of CO_x. In accordance to our earlier suggestions of alkoxides as precursors to combustion [13], it is possible that in the P_Li/MgO system, the presence of new [O^-] defect sites created from the photo-excitation

Table 1 Selectivity to various products with Li/MgO in the absence and the presence of plasma

	Li/MgO	P_Li/MgO	Li/MgO	P_Li/MgO
T (°C)	500		600	
Selectivity (mol%)				
COx	75.0	30.5	28.4	19.0
$C_1°$–$C_5°$	0.8	5.1	9.3	16.9
C_2H_2	–	16.7	–	0.4
$C_2^=$–$C_5^=$	21.2	43.9	62.3	63.7
C_6^+	3.0	3.8	–	–

Reaction conditions: 100 ml/min, 10% hexane, 8% oxygen and balance helium. WHSV = 3.08 h^{-1}

of the O^{2-} sites of MgO, minimizes the unselective interaction of radicals with the latter for alkoxide formation, thus minimizing combustion.

Results discussed above indicate that combination of plasma and Li/MgO catalyst during the oxidative conversion of hexane is advantageous resulting in significantly higher hexane conversions and higher selectivities to olefins. However, it is crucial to investigate the contribution of the catalyst surface in both hexane activation and olefin formation when plasma chemistry is occurring.

At 500°C, the similarity in hexane conversions with both the catalyst and quartz systems (Fig. 6) indicates less significant contribution from the catalyst in hexane conversion at this temperature. The higher conversions achieved with the presence of a dielectric material (Li/MgO catalyst and quartz inert) compared to the plasma reactor (P_ER), is thus due to accelerated gas phase chemistry as result of increase in both permittivity and electron energy with the introduction of the packing material. However, at 600°C, hexane conversion from the P_Li/MgO was significantly higher than that from P_Quartz system. This indicates that at this temperature there is more contribution from the catalytic defect sites ($[O^-]$) in hexane activation.

Figure 7 presents the product distribution from the oxidative conversion of hexane at 500°C in the systems: (1) plasma empty reactor (P_ER), (2) plasma- Li/MgO (P_Li/MgO) and (3) plasma-quartz inert (P_Quartz). Compared to both P_ER and P_Quartz systems, P_Li/MgO resulted in less formation of C_6^+ products, and more of combustion products. This is mainly explained, as discussed earlier, by the unselective interaction of intermediate radicals with the O^{2-} sites of MgO, enhancing combustion and minimizing coupling reactions. Both the catalyst and quartz systems resulted in significantly higher C_2H_2 formation than the empty reactor. It is reported by Kado et al. [22] that extent of C_2H_2 formation depends on the concentration of CH radicals; thus depends on the extent of dissociation and dehydrogenation reactions via electron impacts. In agreement, the high selectivities to C_2H_2 observed for both catalyst and quartz systems are due to the increase in extent of electron impact excitations as result of increase in permittivity and electron energy with the introduction of the packing material.

The olefin distribution, i.e., $(C_2H_2 + C_2H_4) > (C_3^=\text{-}C_5^=)$ for the above three systems (Fig. 7) strongly suggests that at this temperature plasma chemistry is more dominant.

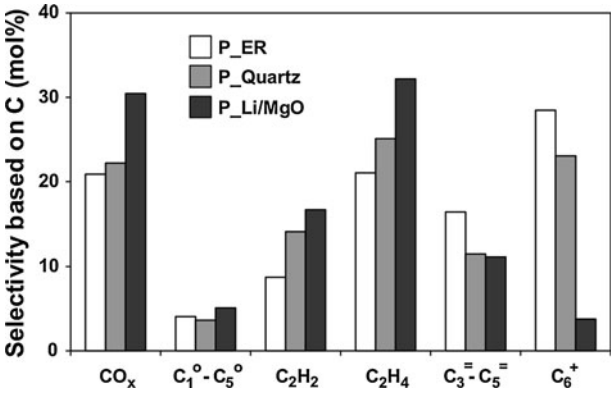

Fig. 7 Product distribution of oxidative conversion of hexane at 500°C, with (1) P_ER (2) P_Quartz and (3) P_Li/MgO systems. Reaction conditions: 100 ml/min, 10% hexane, 8% oxygen and balance helium. WHSV = 3.08 h^{-1}

Further, to gain insight on the contribution of Li/MgO catalyst in hexane activation and in controlling olefin formation, a different reactor configuration with Li/MgO downstream to plasma (Fig. 1.d) was investigated and compared to gas phase non-catalytic reactions in an empty reactor as in Fig. 1c. Results of experiments with this reactor configuration at 500°C (Table 2) confirm the low contribution of the catalyst in hexane activation and in olefin formation. At this temperature the catalyst downstream to plasma (PB_Li/MgO) showed slightly lower hexane conversion due to quenching and similar selectivity to C_2-C_5 olefins, compared to the plasma reactor in absence of the catalyst (P_ER) (Fig. 1c). Thus, at 500°C, plasma chemistry is more dominant, where hexane activation in gas phase via electron impact excitations and collisions with $O(^3P)$ atoms (1–7) is a more significant pathway.

Figure 8 presents the product distribution at 600°C of the three systems: (1) plasma empty reactor (P_ER), (2) plasma- Li/MgO (P_Li/MgO) and (3) plasma-quartz inert (P_Quartz). Similar as in P_ER, acetylene formation in the P_Li/MgO system was minimal mainly due to complete oxygen consumption (O_2 conversion = 100%). In the quartz system, as oxygen was not completely consumed (O_2 conversion = 97 mol %), C_2H_2 formation was still observed. We speculate that in oxygen depleting conditions, hence in absence of $HO_2^{\bullet}$ chain propagators, $CH^{\bullet}$ radicals act as the main chain propagators and react further with intermediate radicals enhancing olefin formation.

Table 2 Influence of catalyst downstream to plasma zone

	P_ER	PB_Li/MgO
Conversion (mol%)		
C_6H_{14}	23.2	20.3
O_2	72.1	92.3
Selectivity (mol%)		
CO_x	20.0	54.7
C_1^o–C_5^o	2.3	3.6
C_2H_2	5.3	10.5
$C_2^=$–$C_5^=$	30.1	31.2
C_6^+	42.3	–

Reaction conditions: 100 ml/min, 10% hexane, 8% oxygen and balance helium. WHSV = 5.1 h^{-1}, T = 500°C

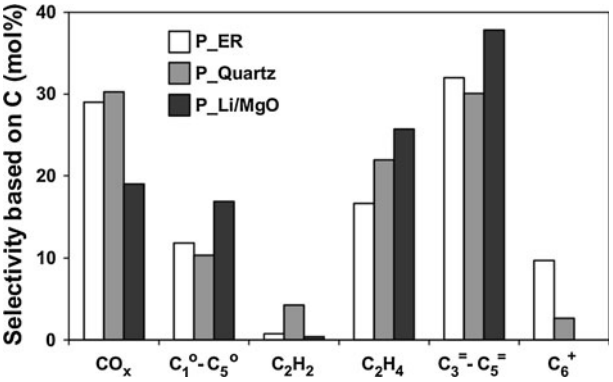

Fig. 8 Product distribution of oxidative conversion of hexane at 600°C, with (1) P_ER, (2) P_Quartz and (3) P_Li/MgO systems. Reaction conditions: 100 ml/min, 10% hexane, 8% oxygen and balance helium. WHSV = 3.08 h^{-1}

Table 3 Influence of catalyst downstream to plasma zone

	P_ER	PB_Li/MgO
Conversion (mol%)		
C_6H_{14}	30.5	38.0
O_2	99.4	99.3
Selectivity (mol%)		
CO_x	27.8	26.1
C_1^o–C_5^o	7.2	8.1
C_2H_2	1.3	1.0
$C_2^=$–$C_5^=$	48.2	64.8
C_6^+	15.6	–

Reaction conditions: 100 ml/min, 10% hexane, 8% oxygen and balance helium. WHSV = 5.1 h^{-1}, $T = 600°C$

Scheme 1 Mechanism of hexane cracking via [O^-] sites of Li/MgO at 600°C

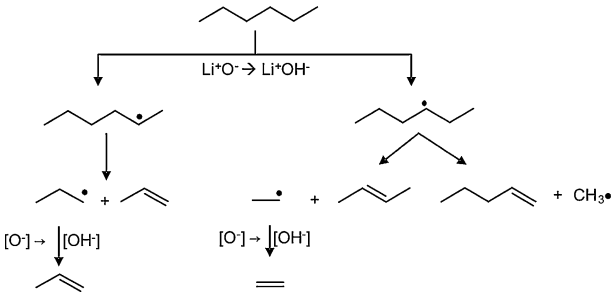

Generally at this temperature more of C_3–C_5 olefins than ethylene was observed with all the systems, i.e., ($C_3^=$–$C_5^=$) > C_2H_4. The P_Li/MgO system, however, resulted in considerably higher formation of C_3-C_5 olefins (38 mol%) than P_ER (32 mol%) and P_Quartz systems (30 mol%). This indicates the role of the Li/MgO in enhancing C_3–C_5 olefin formation.

Further, experiments with Li/MgO downstream to plasma (PB_Li/MgO) at 600°C (Table 3) showed higher hexane conversion and significantly higher C_2–C_5 olefins (64 mol%) than with the P_ER (48 mol%). The higher selectivity to olefins suggests consecutive interaction of alkyl radicals formed in the plasma with the active sites of Li/MgO, abstracting a second hydrogen atom from the alkyl radical forming an olefin.

Thus at 600°C, even in presence of plasma, the surface chemistry of Li/MgO becomes significant; i.e., (1) hexane activation via the [Li^+O^-] defect sites, forming iso-hexyl radicals, which through β-scission yield C_3-C_5 olefins, and (2) consecutive interaction of intermediate radicals with the [O^-] defect sites of the catalyst leading to more olefin formation. A simplified mechanism for hexane cracking via [O^-] sites of Li/MgO at 600°C is illustrated in scheme 1.

Optimal Reactor Configuration for the Oxidative Conversion of Hexane

The integrated plasma-Li/MgO system is the optimal reactor configuration with the highest yields of C_2–C_5 olefins, as shown in Fig. 9. The introduction of the catalyst in the plasma system results in an increase in both electron density and energy; thus the number of electron impact excitations increases, leading to improved hexane conversions. Moreover, UV light from plasma creates new [O^-] defect sites on the catalyst surface, enhancing activity and minimizing combustion reactions.

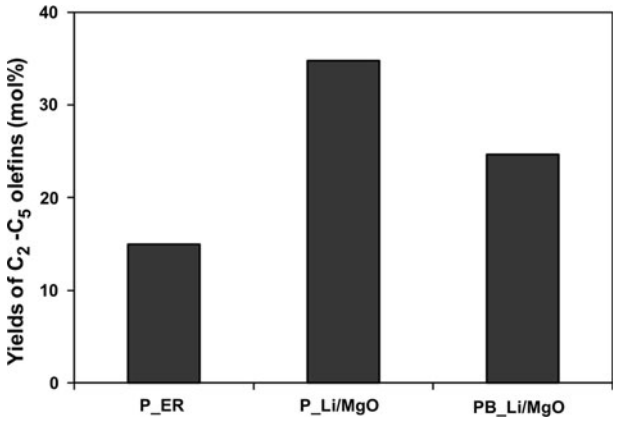

Fig. 9 Yields of C_2–C_5 olefins with different reactor configurations. Reaction conditions: 100 ml/min, 10% hexane, 8% oxygen and balance helium. $T = 600°C$

Table 4 Estimated energy for integrated plasma-Li/MgO

BDE, 2ndary C–H (KJ/mol)	Hexane converted (mol/min)	Energy needed (J/min)	Energy absorbed by plasma (J/min)	Energy loss (%)
394	1.38E−04	54	180	70

In order to explore the potential for industrial application of the integrated plasma-Li/MgO system, an estimation of the energy efficiency of the system was attempted. Table 4 shows a qualitative estimate of the energy efficiency of the integrated plasma-Li/MgO system. The amount of the energy absorbed by plasma (180 J/min) was compared to the amount of energy needed for dissociation of the C–H bond in the converted hexane (54 J/min). Results indicate that only 30% of energy absorbed by plasma is utilized for hexane conversion. Inefficient utilization of plasma energy, thus, strongly suggests that further improvement in the energy efficiency of the system is required.

Conclusion

Application of both plasma and Li/MgO catalyst in oxidative conversion of hexane results in considerable improvements both in hexane conversions and selectivities to light olefins ($C_2^=$–$C_5^=$) at a relatively low temperatures of 500–600°C. The yields of olefins achieved with the integrated plasma-Li/MgO-catalyst are considerably higher than those achieved with Li/MgO in absence of plasma or in plasma reactor in absence of catalyst.

The combination of plasma and catalyst results in synergy. (1) Presence of plasma creates new [O^-] defect sites in the catalyst. These enhance hexane activation and moreover minimize the unselective interaction of radicals with O^{2-} sites of MgO resulting in alkoxide formation, hence minimize combustion. (2) The presence of the Li/MgO catalyst in the plasma reactor, results in an increase in both electron-density and -energy, leading to enhanced electron impact dissociations of hexane and oxygen molecules.

In the integrated plasma-Li/MgO system hexane activation takes place via three main routes; (1) C–H bond scission via the $[O^-]$ defect sites originally present as $[Li^+O^-]$ as well as created via photo-excitation of O^{2-} sites of MgO, (2) C–C, C–H bond scission by electron-impact excitation of hexane molecule with electrons, and (3) C–H bond scission by $O(^3P)$ oxygen atoms formed from collisions of oxygen molecules with electrons.

Temperature influences the performance of the integrated plasma-Li/MgO system, as illustrated by the differences in the product distribution at both temperatures. At 500°C, significant formation of acetylene and ethylene and low formation of the high olefins ($C_3^=$–$C_5^=$) was observed. It is proposed that at this temperature plasma chemistry is more dominant. Acetylene formation is a characteristic of plasma chemistry, and can be formed via dimerization of CH species formed in the presence of plasma and through the extensive dehydrogenation of ethane.

At 600°C, the reaction of intermediate radicals with oxygen to from olefins, is more favored, hence more formation of the high olefins was observed, i.e., ($C_3^=$–$C_5^=$) > C_2H_4. At this temperature the contribution of Li/MgO catalyst in hexane activation and enhancing olefin formation becomes more significant. The absence of acetylene at this temperature together with oxygen depletion, suggest that oxygen depleting conditions are required to minimize acetylene formation.

Despite the significant improvements achieved with the application of plasma in the yields of C_2–C_5 olefins, the integrated plasma-Li/MgO system still can not compete with the conventional cracking processes, due to the low energy efficiency.

Acknowledgments The authors gratefully thank ASPECT program, the Netherlands, for financial support (project number 053.62.011). The authors also acknowledge Ing. B. Geerdink and K. Altena-Schildkamp for technical support, L. Vrielink for BET measurements.

References

1. Lin C-H, Campbell KD, Wang J-X, Lunsford JH (1986) J Phys Chem 90:534
2. Driscoll DJ, Martir W, Lunsford JH (1987) J Phys Chem 91:3585
3. Ito T, Wang J-X, Lin C-H, Lunsford JH (1985) J Am Chem Soc 107:5062
4. Xu M, Shi C, Yang X, Rosynek MP, Lunsford JH (1992) J Phys Chem 96:6395
5. Morales E, Lunsford JH (1989) J Catal 118:255
6. Cavani F, Trifiro F (1995) Catal Today 24:307
7. Landau MV, Kaliya ML, Gutman A, Kogan LO, Herskowitz M, van den Oosterkamp PF (1997) Stud Surf Sci Catal 110:315
8. Leveles L, Seshan K, Lercher JA, Lefferts L (2003) J Catal 218:307
9. Leveles L, Seshan K, Lercher JA, Lefferts L (2003) J Catal 218:296
10. Trionfetti C, Babich IV, Seshan K, Lefferts L (2006) Appl Catal A 310:105
11. Trionfetti C, Babich IV, Seshan K, Lefferts L (2008) Langmuir 24:8220
12. Cavani F, Ballarini N, Cericola A (2007) Catal Today 127:113
13. Boyadjian C, Lefferts L, Seshan K (2010) Appl Catal A 372:167
14. Trionfetti C, Agiral A, Gardeniers JGE, Lefferts L, Seshan K (2008) Chem Phys Chem 9:533
15. Trionfetti C, Agiral A, Gardeniers JGE, Lefferts L, Seshan K (2008) J Phys Chem 112:4267
16. Agiral A, Boyadjian C, Seshan K, Lefferts L, Gardeniers JGE (2010) J Phys Chem C 114:18903
17. Ahmed S, Aitani A, Rahman F, Al-Dawood A, Al-Muhaish F (2009) Appl Catal A 339:1
18. Harling AM, Demidyuk V, Fischer SJ, Whitehead JC (2008) Appl Catal B 82:180
19. Zhu X, Huo P, Zhang Y-P, Cheng D-G, Liu C-J (2008) Appl Cat B 81:132
20. Nozaki T, Muto N, Kado S, Okazaki K (2004) Catal Today 82:57

21. Kangjun W, Xiaosong L, Hui W, Chuan S, Yang X, Amin Z (2008) Plasma Sci Tech 10:600
22. Kado S, Urasaki K, Sekine Y, Fujimoto K, Nozaki T, Okazaki K (2003) Fuel 82:229
23. Aika K-I, Lunsford JH (1977) J Phys Chem 81:1393
24. Aika K-I, Lunsford JH (1978) J Phys Chem 82:1794–1800
25. Kondratenko EV, Sinev MY (2007) Appl Catal A 325:353
26. Sterrer M, Berger T, Diwald O, Knozinger E (2003) J Am Chem Soc 125:195
27. Sterrer M, Diwald O, Knozinger E, Sushko Peter V, Shluger Alexander L (2002) J Phys Chem B 106:12478
28. http://clippercontrols.com/info/dielectric_constants.html#M
29. http://farside.ph.utexas.edu/teaching/em/lectures/node100.html
30. Xu X (2001) Thin Solid Film 390:237
31. Li R, Tang Q, Yin S, SatoT (2006) Fuel Process Technol 87:617
32. Kang WS, Park JM, Kim Y, Hong SH (2003) IEEE Trans Plasma Sci 31:504